RESEARCH PAPER

Extraction-preconcentration Mercury ion by *Ghezeljeh* montmorillonite nanoclay as a new native adsorbent from food and water samples

Zahra Hassanzadeh Siahpoosh*, Majid Soleimani [1,2]

Department of Chemistry, Imam Khomeini International University (IKIU), Qazvin, Iran

ARTICLE INFO

Article History:
Received 02 October 2016
Accepted 24 December 2016
Published 15 January 2017

Keywords:
Adsorption
Clay
Food
Mercury
Water

ABSTRACT

Ghezeljeh montmorillonite nanoclay or "*Geleh-Sar-Shoor*" (means head-washing clay) used as a native adsorbent to extraction-preconcentration mercury ions from a variety of real water and fish samples have been investigated in a batch system followed by atomic absorption spectroscopy (AAS) with vapor generation accessory (VGA) system. The clay was characterized by using FT-IR, SEM-EDS, XRF, XRD, CEC, Specific surface area and Zeta potential. The results of XRD, FT-IR, Zeta potential and CEC of the *Ghezeljeh* clay confirm that montmorillonite is the dominant mineral phase. On the basis of on SEM images, the distance between the layers is in nm level. The outcome of varying parameters and interfering ions were studied. Detection and quantification limits, preconcentration factor, and adsorption capacity were calculated. The Langmuir and Freundlich equations showed the finest fit to the equilibrium data. The adsorption procedure follows a pseudo-second-order reaction pattern. Calculation of ΔG^0, ΔH^0 and ΔS^0 displayed that the nature of Hg(II) ions adsorption is endothermic and favorable at upper temperature.

How to cite this article
Hassanzadeh Siahpoosh Z, Soleimani M. Extraction-preconcentration Mercury ion by Ghezeljeh montmorillonite nanoclay as a new native adsorbent from food and water samples. Nanochem Res, 2017; 2(1): 42-59. DOI: 10.22036/ncr.2017.01.005

INTRODUCTION

Heavy metal pollution is produced throughout manufacturing and farming doings, and furthermore is realized in vehicular productions. Mercury ion is one of the most severe contaminants of heavy metals in water and sediment, upcoming from chlor-alkali business, medicinal, paper, oil factory, dye, and battery activities. Heavy metals are nonbiodegradable, consequently removal of heavy metal ions from water and wastewater is very important [1-3]. Up to now, the progress of analytical systems for the specification the amount of mercury has been a difficult task. A severe trouble faced in the specification the amount of mercury is that goal types generally exist in small concentrations. A lethal concentration of mercury salts covers from less than 0.1 ng/ml to further than 200.0 ng/ml for aquatic types and river creatures. Diverse types of ways are obtainable for eliminating mercury in water and wastewater containing electrodialysis, conventional coagulation, chemical precipitation, reverses osmosis, line softening, photocatalytic reduction, ion-exchange, adsorption [2-5]. Amongst these procedures, adsorption is an extremely operational, inexpensive, and commonly practical way. Definite adsorption of mercury ion by diverse kinds of low price farming waste ingredients such as tree bark, peanut skin, wool, onion skin, sawdust and coconut husk and manufacturing waste ingredients for example rubber, waste tyre, enricher waste slurry, coal, and photofilm waste slurry has been informed [2]. Most recently, many classes of clay minerals have been used as adsorbents to remove pollutants from wastewater [3]. Clay

* Corresponding Author Email: *z.hassanzadeh.s@gmail.com*

minerals have drawn greatly consideration because of their characteristic structures; for example its great specific surface area, swelling, ion exchange properties, high sorption capacity, intercalation behavior and their smaller price paralleled to synthesized ingredients (e.g. silica gel, zeolite) [6]. This paper is a report on a research trying to extract and preconcentrate mercury ions from aqueous solutions using batch equilibrium technique by *Ghezeljeh* montmorillonite nanoclay as natural and native adsorbent. It is worth nothing that *Ghezeljeh* montmorillonite nanoclay (*Geleh-Sar-Shor*) was used in ancient Persia to clean the body, hair, and also to bathe dead bodies prior to the funeral ("*Geleh-Sar-Shoor*" means head-washing clay). The clay is still used in some parts of Iran. This clay is readily obtainable, low-priced and environmentally friendly with chemical and mechanical stability. *Ghezeljeh* clay is distinguished by using Fourier transform infrared spectroscopy (FT-IR), scanning electron microscopy-energy dispersive spectrometer operating (SEM-EDS), X-ray diffractometry (XRD), X-ray fluorescence (XRF), cation exchange capacity (CEC) measurements, specific surface area and zeta potential. The results of XRD, FT-IR, zeta potential and CEC of *Ghezeljeh* clay confirm that montmorillonite is the dominant mineral phase. On the basis of SEM images of clay, the distance between the layers is in nm scale. The current study overlaid the use of Dubinin–Radushkevich, Temkin, Langmuir and Freundlich isotherm models to define the adsorption progression onto nanoclay. Kinetic models such as first-order, second-order equations and intra-particle diffusion model and thermodynamics were moreover studied. So far, *Ghezeljeh* montmorillonite nanoclay (*Geleh-Sar*-Shoor) has not been studied as an adsorbent for the extraction-preconcentration of heavy metals. Only Soleimani and Hassanzadeh in the Imam Khomeini International University (IKIU) have used *Geleh-Sar*-Shoor for the extraction of metal ions [7-9].

Theoretical Considerations

Clay

Clays are hydrous aluminum silicates which are ordered as 1:1 and 2:1 clay minerals. The sheets in these clays are kept up by weak van de Waals forces making it easy for other compounds to take up the interlayer region. Montmorillonite is dioctahedral clay of the smectite type including alumino-silicate layers. The silica tetrahedra (T) (Si^{4+} in tetrahedral coordination with O^{2-}) and alumina octahedral (O) (Al^{3+} in octahedral coordination with O^{2-}) are interrelated (through the sharing of O^{2-} at polyhedral corners and edges) in such a fashion that a sheet of alumina octahedral is inserted between two sheets of silica tetrahedral. Consequently, the configuration is T-O-T (2:1) [10]. Most of the surface charges on montmorillonite are created by isomorphous replacement or non-ideal octahedral possession. Adsorption of metal cations in clay minerals is restricted by factors such as charge features of the clay. Charge features contain the amount of the active places and cation exchange aptitude. The exchange progressions depend on several elements, similar the physicochemical features of solid and cation (such as ionic radius, charge extent, hard–soft acid–base characteristics, hydration volume and hydration enthalpy of cation), temperature, ionic power, concentration of ions, existence of challenging ions, and experimental situations involving time of reaction, and pH of the medium [11-18]. The information of the heavy metal binding to the mineral building is of main importance to calculate the motion and long-term behavior of heavy metals in natural structures [19].

Metal sorption mechanisms onto montmorillonite

Although numerous examinations on metal adsorption on montmorillonite have been successfully exhibited, there is no entire agreement on adsorption locations, surface responses and exhibiting methods. It is consequently challenging to differentiate the adsorption affinity of numerous metal cations by montmorillonite. Through the dissimilar nature of the clays, it is probable that numerous metal sorption mechanisms happen at the same time creating the determination of metal/clay factor interaction problematic on such substance [1,6,19]. Brigatti et al. [1] have reported that mercury is specially adsorbed as Hg–OH complexes in montmorillonite. Hg–OH_2 complexes are fewer powerfully linked to the 2:1 sheets, as verified by EXAFS and thermal study. On the opposing, Hg–O intercalates are further toughly bounded to the layers and mercury is released at upper temperatures. Sajidu et al. [6] have studied the interactions of copper(II), cadmium(II), zinc(II), mercury(II), chromium(III), and lead(II) on natural basic variegated clays using EXAFS spectroscopy. Mercury(II) is adsorbed as hydrolyzed lined O–Hg–O elements on the clay surface at neutral pH, whereas it is reduced to mercury(I) at low pH and adsorbed as ≡O–Hg–Hg–OH_x complexes (x = 1 or 2). The adsorption of metal ions chiefly relies on its hydrated radius [20-22]. The metal ions having lesser hydrated ionic radius have easier contact to the mineral's surface and can diffuse more simply inside its openings. On the other hand, the existence of ions having a higher hydrated ionic radius outcome an extra quick overburden of the adsorption locations [23].

MATERIALS AND METHODS

Reagents and solutions

All the chemicals were purchased from the German company of Merck: acids, bases, hydrogen peroxide, sodium acetate, sodium carbonate, sodium citrate, nitrate salts of copper, lead, chromium, cobalt, cadmium, mercury, sulfate salts of aluminum, nickel, manganese, zinc, magnesium, chloride salts of sodium, potassium, iron, calcium, and ammonium. Since the chemicals were at the maximum purity, they were applied without any purification. The element standard solutions were produced by diluting a stock solution of 1000 mg/l of the specified component using doubly distilled water. The Hg(II) stock aqueous solution (1000 mg/l) was obtained from the dissolution of Mercury(II) nitrate monohydrate (Merck, Darmstadt, Germany), acidified with nitric acid to avoid Hg precipitation. The employed solutions of Hg(II) ions were readied day-to-day via suitable dilution of mercury stock solution which was prepared weekly. A citrate-citric acid buffer solution was readied using 0.1 M citric acid solution at pH 2-3. Acetate buffer solution was readied via combining suitable volumes of 0.1 M acetic acid and 0.1 M sodium acetate at pH 4-6. Phosphate buffer solution was readied by 0.1 M phosphoric acid at pH 7. Carbonate buffer solution was readied using 0.1 M sodium carbonate at pH 7. Citrate buffer solution was readied using 0.1 M sodium citrate at pH 7. Ammonium buffer solution was readied by mixing suitable quantities of 0.1 M ammonia and 0.1 M ammonium chloride at pH 8-10. The pH of the buffer solutions was balanced by adding 1 M NaOH or HCl, as needed. The *Ghezeljeh* montmorillonite clay (adsorbent) was collected from *Ghezeljeh*, a village 18 km west of the city of Tafresh (Markazi Province) in Iran. Different water samples used in the experiments were collected from Caspian Sea, Karun River (inside and outside the city of Ahvaz), Persian Gulf, Iran, Well water, Haryrood river, and Tap water (from *Herat* city), Afghanistan. Five different fresh fish samples used in the experiments were obtained from the local markets in *Qazvin*, Iran.

Instrumentation

A model 420A digital Orion pH meter (Gemini, the Netherlands) prepared by a combined glass electrode was applied for pH corrections. An ultrasonic water bath (Bandelin, Berlin, Germany) was used to disperse and disaggregate this clay. Batch experiments were carried out in Incubator Shaker (model 3020 DRS, FSA, Iran) at 200 rpm in Imam Khomeini International University (IKIU). X-Ray diffraction (XRD) data were attained by an Ital Structures diffractometer (GNR, Novara, Italy), with Cu K_α radiation (40 kV/30 mA, λ= 1.542 A°). Fourier transform infrared (FT-IR) examine was applied by Tensor Bruker MIR-T27 (Germany) taking a standard mid-IR DTGS detector in IKIU. To quantitatively measure the mercury ions in the standard solutions, a GBC 902 flame atomic absorption spectrometry (FAAS), (Dandenong, Victoria, Australia 3175) with deuterium background corrector and an air-acetylene flame was used in IKIU. The working situations in the FAAS spectrometer were adjusted according to the standard procedures of the company. However, the analysis of natural water and fish samples were achieved with a Varian 220Z (Australia) atomic absorption spectrometer (AAS) with vapor generation accessory (VGA) system was used in Iran mineral processing research center (IMPRC). Philips X-ray fluorescence (XRF) of the sample was carried out using XRF analysis instruments (Philips Magix Pro, Netherlands) in IMPRC. A scanning electron microscope (SEM) (LEO 1450 VP, Thornwood, N.Y., USA) by variable pressure secondary electron detector and energy dispersive spectrometer operating (EDS) at 30 kV (Oxford INCA software, High Wycombe, U.K.) were applied for SEM-EDX analysis in IMPRC. Zeta potential measurements were carried out on a Zetameter ZetaCAD (CAD Instruments, France) in Islamic Republic of Iran Ministry of Agriculture-Jahad. The specific surface areas were calculated by the BET method by means of a Belsorp mini II instrument (BelJapan, Japan) in University of Tehran.

Preparation of the adsorbent

The adsorbent was readied using the *Galehouse* method [7-9]. Natural *Ghezeljeh* clay was first treated with 0.1 M of acetic acid to eliminate carbonates, and then 30% H_2O_2 was used to exclude mineral and organic impurities. The clay was carefully rinsed with doubly distilled water to eliminate traces of acetic acid and hydrogen peroxide. The treated clay was dispersed and disaggregated in doubly distilled water through an ultrasonic water bath. The resulting suspension was transferred to a measuring cylinder and permitted to stand for 3 h, 26 min, 6 sec for sedimentation. The fine fraction (< 2 μm) was removed and placed in an electric vacuum oven at 50°C for 72 h to be dried. Then, it was placed in a desiccator for subsequent experiments.

Adsorption way

Studies on adsorption process were performed through batch method at room temperature. At first, a 50 ml solution containing mercury was moved into an Erlenmeyer flask. Then, 10 ml of an appropriate buffer solution was added and followed by 0.5 min of agitation. Next, 2 g of the *Ghezeljeh* clay was added. The mixture was agitated for 10 min using a mechanical shaker. The liquid phase was separated from the solid part via centrifugation at 3500 rpm for 30 min. The supernatant was decanted.

Desorption way

To elute the analytes adsorbed onto the *Ghezeljeh* clay, 10 ml of 3M HCl was added to the solid part, then it was stirred for less than 0.5 min. The suspension was allowed to stand for 20 min. Then, it was centrifuged at 3500 rpm for 30 min. The supernatant (10 ml) was collected to measure its mercury ion concentration. To optimize the experimental conditions, these steps were repeated three times. The equivalent method was used to the blank solution.

Physicochemical characterization of Ghezeljeh nanoclay

SEM study

Scanning electron microscopy (SEM) is a powerful technique applied in micro imaging of a variety of surfaces. Clay samples were covered with Au under vacuum in an argon atmosphere. Solid morphology; particle size and texture of the clay surface were determined by scanning electron microscopy (SEM) studies (Fig. 1a). On the base of SEM images of clay, the distance between the layers is in nm level, as shown in Fig. 1.

XRD study

X-ray diffractograms were obtained for the 2θ angles ranging from 2° to 40° 2θ at room temperature. The clay was treated with ethylene glycol, an organic compound which steadily intercalates itself into the lattice of the clay. The structural possessions of the clay were monitored beforehand and afterward treatment with ethylene glycol. The X-Ray diffraction analysis revealed that the clay sample was chiefly made up montmorillonite minerals (Fig. 1b) [10,24,25]. The strong 13.69, 5.26

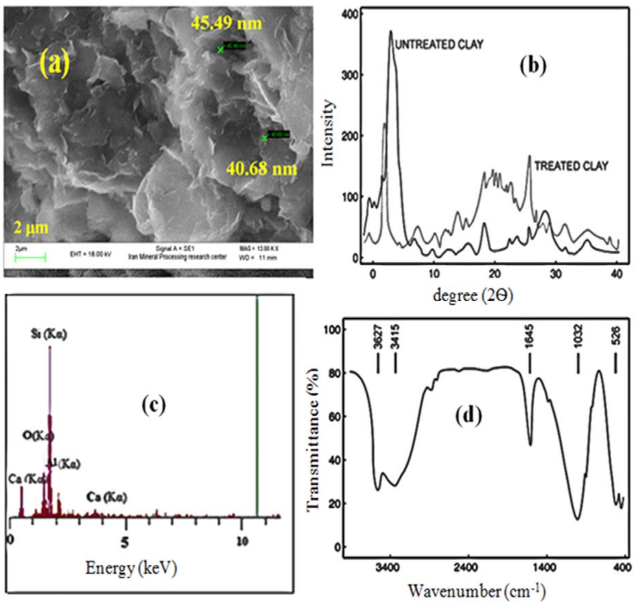

Fig. 1. (a) SEM images, (b) The XRD patterns of the *Ghezeljeh* nanoclay treated with ethylene glycol, (c) EDX spectrum, (d) FT-IR spectrum of untreated *Ghezeljeh* nanoclay.

and 3.27 Å peaks and relatively weak 9.50 Å peak in ethylene glycol-solvated case are related to mixed-layered illite/smectite. Using 9.50 (001/002 Ill/S) and 5.26 Å (002/003 Ill/S) peaks, the estimated percent of illite in the mixed-layered. The 7.30 and 3.61 Å peaks indicate that kaolinite is also present [26].

XRF and EDS study

The chemical composition of this clay was determined with XRF and EDS (Fig. 1c). Results of XRF analysis: SiO_2: 54.47; Al_2O_3: 20.92; MgO: 3.65; SO_3: 0.32; K_2O: 1.82; CaO: 1.14; Na_2O: 0.16; TiO_2: 0.37; Fe_2O_3: 3.13; PbO: 0.16; SrO: 0.10; ZrO_2: 0.05; As_2O_3: 0.02; Loss-on-ignition corrections (L.O.I.): 13.7.

FT-IR study

To prepare the clay sample for FT-IR spectroscopy, an electric vacuum oven was used to dry (at 50°C for 6 h) and cool the clay. A FT-IR spectrum was indicated in the range of 400-4000 cm^{-1} with the KBr pellet method. Mixed-layered illite/smectite is distinguished according to the absorption bands near 3627 and 1029 cm^{-1}, bands near 914 and 836 cm^{-1}. Sharp bands at 3694 and 3927 cm^{-1} belong to kaolinite [26]. The FT-IR analysis, also confirmed that the *Ghezeljeh* montmorillonite clay is mainly composed of montmorillonite minerals (Fig. 1d) [10].

Cation exchange capacity (CEC)

The cation exchange capacity (CEC) is the amount of equals of interchangeable charge per quantity of clay, which is equal with the layer charge [27]. The CEC of the *Ghezeljeh* montmorillonite nanoclay was calculated with 0.01 M Cu-triethylentetramine [28,29]. The CEC value of 160.0 meq/100 g for *Ghezeljeh* montmorillonite nanoclay was found. The significant value of CEC is in a good agreement with what has been reported for Montmorillonite in the literature [30].

Surface area

The specific surface area (S_{BET}), pore radius and pore volume of the *Ghezeljeh* montmorillonite nanoclay were obtained from N_2 adsorption isotherms attained at liquid nitrogen temperature (at 77 K) by means of a Belsorp mini II instrument (BelJapan, Japan). Prior to the surface area calculations, humidity and vapor on the solid surface or entered in the open holes were cleaned off by heating under vacuum at 100°C for 12 h. The *Ghezeljeh* montmorillonite nanoclay possesses a specific surface area of 90.916 m^2/g, pore radius of 4.8 nm and pore volume of 0.147 cm^3/g [19,31].

Zeta potential measurement

The zeta potential of the *Ghezeljeh* nanoclay was obtained from electrophoretic mobility measurements at 21.31°C, with Zetameter ZetaCAD instruments). The zeta potential obtained at a natural pH of 5.64 is -25.970 mV equivalents to zeta potentials of montmorillonite (−21.2 mV) [32].

RESULTS AND DISCUSSION

Prior to extraction-preconcentration step of mercury ions from real samples, standard solutions were subjected to optimize a number of operating parameters involved in the extraction-preconcentration of mercury ions. The parameters were quantity of adsorbent, eluent characteristics (type, volume, and concentration), pH of the buffer solutions, buffer type, shaking time, volume of the standard solutions, and initial mercury ions concentration (adsorption capacity). The role of desorption time and centrifugation time was also studied. A summary of the main findings is as follows.

Effect of adsorbent amount

Ten quantity levels of the *Ghezeljeh* montmorillonite clay were studied: 0.1, 0.2, 0.3, 0.4, 0.5, 1, 1.5, 2, 2.5 and 3 g. The standard solution was 60 ml composing of 50 ml of doubly distilled water containing 14.63 mg/l of mercury ions and 10 ml of buffer solution added at pH 7. The adsorption of the Hg(II) ions onto the clay improved as the amount of the *Ghezeljeh* nanoclay was increased. However, the adsorption declined at adsorbent amounts higher than 2 g. Reduction in the adsorption could be explained by the point that when the adsorbent amount is less than 2 g, the mercury ions can simply come into contact with the adsorption positions, while when the adsorbent content exceeds 2 g, the amount of such positions per unit quantity decreases, due to accumulation and flocculation of adsorbent fragments [33-35].

Effect of eluent kind, volume and concentration

To obtain suitable eluent, HCl and HNO_3 solutions were used at various concentrations (1-5 M) with varying volumes (5-15 ml) for the elution of mercury ions adsorbed onto the *Ghezeljeh* nanoclay. The adsorbed ions were readily eluted (desorbed) from the nanoclay only when 10 ml of 3 M HCl was used.

Effect of pH of buffer solutions

To research the effect of pH of the buffer solutions in adsorption of mercury ions onto the *Ghezeljeh* nanoclay, pH was adjusted in the cover of 2 to 8 at room temperature, using buffer solutions given in section reagents and solutions. At pH higher than 8, $Hg(OH)_2$ solid phase was formed, therefore the Mercury maintenance ability reduces. Mercury ions were optimally adsorbed on the *Ghezeljeh* nanoclay at pH 7. For subsequent runs of the experiment, pH 7 was applied as the optimum pH level for phosphate buffer solution. The results are shown in Fig. 2a. Clays are identified to have a negative surface charge in solution, as pH changes, surface charge also changes, and the adsorption of charged species is affected. At low pH values, there are extra H_3O^+ ions in solution, a competitiveness occurs between the positively charged hydrogen ions and metal ions for the accessible adsorption positions on the negatively charged clay surface.

Effect of the type of buffer solutions

Three types of buffer solutions were compared at a concentration of 0.1 M at pH 7 in terms of their effect on mercury ions adsorption: phosphate, carbonate and citrate buffer solutions. The phosphate buffer solution led to a higher level of mercury ions adsorption. The percentage of the recovery of mercury ions was approximately consistent with 47.1%, using carbonate and citrate buffer solutions.

Effect of the concentration and pH of phosphate buffer solution

To understand the effect of concentration and pH of phosphate buffer solution on adsorption mercury ions on the nanoclay, concentrations of phosphoric acid in the range of 0.001 M to 3 M and pH from 5 to 8 at room temperature are changed. The maximum percentage of recovery is obtained at 0.1 M and pH 7.

Effect of agitation time

To study the effect of agitation (shaking) time (or contact time), the adsorption of mercury ions onto the *Ghezeljeh* nanoclay was measured after 10, 20, 30, 40, 50 min of shaking the standard solutions (Fig. 2b). It was completed after 20 min adsorption. Consequently Hg(II)–clay interactions arrived at balance state in less than 20 min. It showed that the adsorption locations on the clay minerals were quickly covered using the mercury ion. On the basis of the consequences, a 20 min of agitation

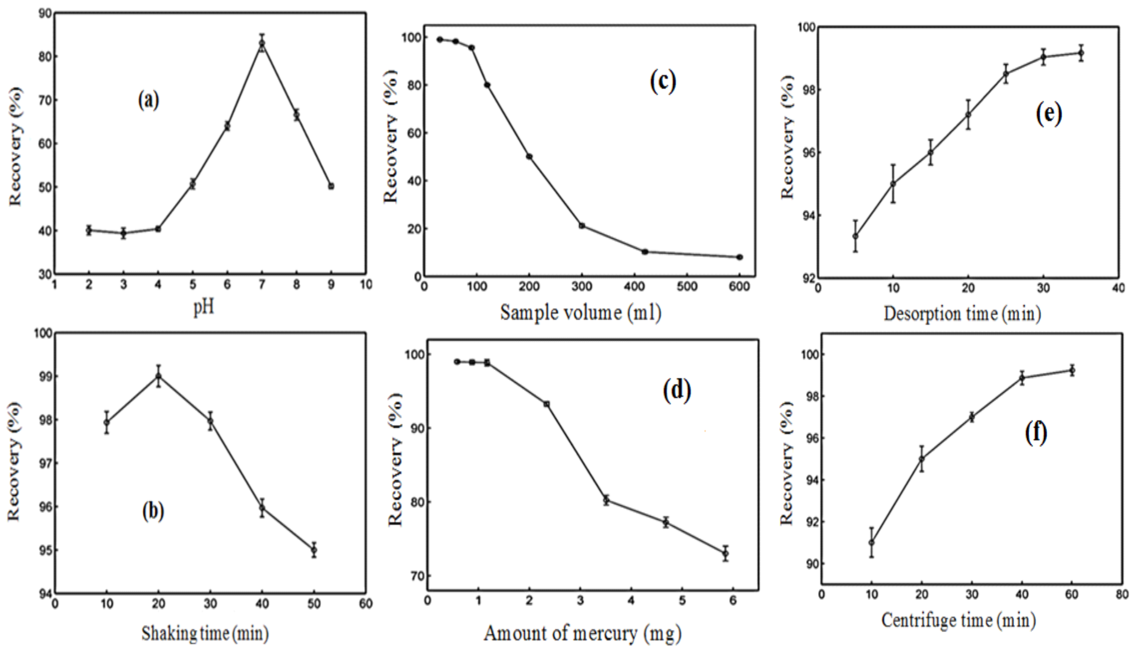

Fig. 2. Effect of (a) pH buffer solution, (b) shaking time, (c) sample volume, (d) initial metal ion concentration (adsorption capacity), (e) desorption time, and (f) centrifugation time on the recoveries of analytes.

time was attained appropriate for the extreme adsorption. This optimum value was used in the rest of experiments.

Effect of volume of standard solutions

To study the influence of the total volume of the standard solution (sample + buffer), on the adsorption of mercury ions onto the *Ghezeljeh* nanoclay, seven quantities of 30, 60, 90, 120, 300, 420, and 600 ml were investigated. This was aimed at attaining a high preconcentration factor. It was found that recovery is over 95% at quantities of 30–90 ml, but it declined to below 95% when the volume of the solution exceeded 90 ml. Now, given that ending solution volume to be determined by FAAS is 10 ml, the preconcentration factor is 9. The results are recorded in Fig. 2c.

Effect of primary mercury ion concentration

The adsorption capacity of an adsorbent is defined as the largest amount of metal adsorbed onto 1 g of the adsorbent [34]. In order to evaluate the adsorption capacity of the *Ghezeljeh* nanoclay, 2 g of the clay was added to different standard solutions containing 0.59, 0.88, 1.17, 2.34, 3.51, 4.68, and 5.85 mg of mercury ions (Fig. 2d). The adsorption capacity was evaluated to be 1.17 mg/g (relative error smaller than ±5%). At lesser concentrations, a great number of adsorption positions on the nanoclay are accessible to the metal ions and this condition is improved with elevation of metal ion concentration and the competition for adsorption locations becomes difficult.

Effect of desorption time

Desorption time is defined as the length of time that an eluent is in contact with the adsorbent containing metal ions. The desorption time in this study was studied by measuring the recovery of mercury ions from the clay after 5, 10, 15, 20, 25, and 30 min of contact between HCl and nanoclay (Fig. 2e). Desorption time of 25 min was found to lead to the highest degree of desorption. This value was applied in the remaining experiments.

Effect of centrifugation time

To explore the effect of centrifugation time on the desorption of mercury ions from the clay, aliquots taken from the standard solutions after 25 min of desorption time were centrifuged for 10, 20, 30, 35, and 40 min at a rotation speed of 3500 rpm (Fig. 2f). The highest recovery of mercury ions was obtained at 30 min of centrifugation.

Effect of Interference from other ions

To evaluate the feasible analytical applications of the preconcentration technique current, the consequence of several foreign ions interfering with the trace measurement of mercury ions on nanoclay was examined under the optimized conditions. Ions were considered to be interfering when they produced an error larger than ±5% in the recovery of mercury ions. None of the added ions caused interference.

Figures of merit

The figures of merit for mercury ions in the present study were measured under optimal experimental situations. The limit of detection (LOD) established on three times replication of the standard deviations of the blank solution (k = 3, n = 10) turned out to be 0.033 ng/ml. The value for the limit of quantification (LOQ) was 0.11 ng/ml, preconcentration factor 9, dynamic

Table 1. The results of additional metal ions on the designation of 17.5 μg/mL of Hg(II) ions.

Ion	Added as	Concentration (mg/L) ion	Recovery%	RSD%
Na^+	$NaCl$	75	95	2.8
Ca^{2+}	$CaCl_2$	15	95	2.1
Mg^{2+}	$MgSO_4$	100	95	1.3
K^+	KCl	120	95	2.2
Zn^{2+}	$ZnSO_4$	70	95	1.2
Fe^{3+}	$FeCl_3$	25	95	3.5
Mn^{2+}	$MnSO_4$	20	95	0.9
Al^{3+}	$Al_2(SO_4)_3$	20	95	1.6
Ni^{2+}	$NiSO_4$	80	95	1.8
Cd^{2+}	$Cd(NO_3)_2$	51	95	1.6
Co^{2+}	$Co(NO_3)_2$	60	95	1.9
Pb^{2+}	$Pb(NO_3)_2$	4	95	3.1
Cr^{3+}	$Cr(NO_3)_3$	10	95	1.7
Cu^{2+}	$Cu(NO_3)_2$	7	95	2.6

Note: the measurements were achieved at optimum parameters (N = 3).

linear range (DLR) from 0.11 ng/ml to 22.2 μg/ml, adsorption capacity was calculated to be 1.17 mg/g. On the whole, full recovery (100%) was obtained under the optimized conditions with standard solutions. The interaction between mercury ions and the *Ghezeljeh* nanoclay was rapid, with the equilibrium batch process being attained in less than 10 min, meaning that the interaction was thermodynamically favorable.

Application

The experimental process was exercised to a variety of real water and fish samples.

Water samples

After the parameters involved in the adsorption and desorption steps of mercury ions were optimized, the method used in this research was separately applied to a variety of natural water samples: Caspian Sea, Iran, Karun River (inside and outside the city of Ahvaz), Iran, Persian gulf (20 km away from the coast of Bandar Abbas), Iran, Well water (10 km outside the city of Herat), Afghanistan, Haryrood river (residential area), Afghanistan, Tap water (from Herat city), Afghanistan. Beforehand the examination, the samples were strained through a Whatman blue band filter paper. Prior to the standard addition, pH of the samples was balanced to the best pH level. Spiking tests using multiple standard addition procedure checked trustworthiness. Each natural water sample was spiked with three standard solutions. Mercury ion level was determined by Varian 220Z atomic absorption spectrometer with VGA system. The recovery was explained as the ratio of the concentration of analytes found to the concentration of analytes spiked. The consequences are recorded in Table 2. The recoveries of the added standard solutions were in the cover of 71–101% with low relative standard deviations (less than 2%), which showed that good recoveries can be attained using this way.

Fish samples

The process used in this research was separately employed to five different fish samples: Trout, canned Tuna (Poolak), Persian Gulf Tiger tooth Croaker; Caspian Pike and Caspian Whitefish were purchased from the local markets in Qazvin, Iran. Fish samples were cleaned with distilled water, and made uniform using an electrical mixer and then dried in an electrical oven at temperature of 100°C for 24 h. The dried sample was homogenized again and was stored in polyethylene bottles for subsequent analysis. Samples were digested using wet digestion [36]. One gram was taken from each fish sample. Then, 16 milliliters of a mixture of HNO_3 and H_2O_2 (6:2) was added to each sample. The digestion vessel was heated on the hot plate up to 130°C for 4 h. The sample was permitted to cool. Then, 25 ml of doubly distilled water was increased while stirring. The resulting solution was filtered through Whatman blue band filter paper. Afterwards, appropriate amounts of 4 M sodium hydroxide were added to adjust the pH level. The sample was then diluted using doubly distilled water until it was 50 ml. The digested food samples were poured into an Erlenmeyer flask. Then, Ten mL of the buffer solution was added. After 0.5 min of agitation, 2 g of the *Ghezeljeh* nanoclay was added. Subsequently, the extraction-preconcentration process was performed. The blank digestions were performed in the same way. Mercury ion level was determined by Varian 220Z atomic absorption spectrometer with VGA system. The results are reported in Table 2. A decline in the recovery of mercury ions was observed. However, the recovery percentage was still significant with low relative standard deviations (less than 4%).

Comparison between this research and similar studies

The detection limit (LOD) and preconcentration factor (P.F) of the offered process for extraction of mercury ions have been matched with those of other extraction procedures reported in the literatures, and the results are summarized in Table 3.

Isotherms

Sorption isotherm is the equation or curve that links the metal concentration that has been adsorbed on the solid part by metal concentration in the solution at balance state for definite temperature. Balance state models can be categorized into empirical and mechanistic models. Empirical models cannot show the mechanisms of the sorbate uptake but can be applied to predict the experimental consequences; however the mechanistic models can describe the system mechanisms. Consequently, mechanistic models explain the fundamental interactions that happen between the metal ions in the solution and the charged surface. Empirical models are commonly established on simple mathematical relations between the liquid part equilibrium concentration and the solid part equilibrium concentration [37]. In terms of the balance state investigation, for many cases, the Langmuir equation is in a good correspondence with the investigational data, whereas the Freundlich equation has also been applied to fit the investigational data in numerous cases. Several investigators have also effectively used other isotherm equations, such as the Temkin and Dubinin–Radushkevich (DR) models to expect the adsorption balance [38,39]. Accordingly, in this study, the isotherm data was examined using the Langmuir, Freundlich, Temkin, and Dubinin–Radushkevich equations.

Adsorption isotherm experiments

A sequences of 50 ml glass bottles were filled up with 30 ml of standard solutions composing of 25 ml of doubly distilled water containing primary concentration of mercury ions from 10 to 50 mg/l, and 5 ml of buffer solution added at pH 7,

Table 2. Extraction-preconcentration of Hg(II) ions from water and fish samples.

Sample	Added (µg/mL)	Found (µg/mL)	Recovery%	RSD%
Tap water	-	0.212	-	0.6
	1.200	1.427	101	0.8
	1.900	1.890	88	0.9
	2.700	2.310	78	1.1
Caspian Sea	-	0.075	-	1.7
	1.200	1.210	94	1.5
	1.900	1.890	95	1.7
	2.700	2.100	75	1.9
Karun river (inside city)	-	0.232	-	1.1
	1.200	1.320	90	1.1
	1.900	1.820	83	1.3
	2.700	2.190	72	1.2
Karun river (outside city)	-	0.055	-	1.9
	1.200	1.234	98	1.8
	1.900	1.920	98	1.8
	2.700	2.200	79	1.6
Persian gulf	-	0.011	-	1.2
	1.200	1.167	96	1.4
	1.900	1.560	81	1.8
	2.700	2.100	77	1.2
Well water	-	0.064	-	0.7
	1.200	1.281	101	0.6
	1.900	1.668	84	0.7
	2.700	1.989	71	0.9
Haryrood river		0.179		0.9
	1.200	1.259	90	0.8
	1.900	1.860	88	1.1
	2.700	2.274	77	1.0
Trout fish	-	0.125	-	2.2
	1.200	1.189	88	2.8
	1.900	1.657	80	2.9
	2.700	2.101	73	2.8
Canned Tuna fish	-	0.152	-	3.1
	1.200	1.111	80	3.3
	1.900	1.564	74	3.1
	2.700	2.101	72	3.5
Tiger tooth Croaker fish	-	0.150	-	3.3
	1.200	1.123	81	3.9
	1.900	1.600	76	3.9
	2.700	2.130	73	4.0
Pike fish	-	0.057	-	2.7
	1.200	1.112	88	2.9
	1.900	1.643	83	2.7
	2.700	2.234	80	3.1
Whitefish	-	0.136	-	3.4
	1.200	1.112	81	3.2
	1.900	1.546	74	3.2
	2.700	2.030	70	3.6

Note: the measurements were achieved at optimum parameters (N = 3).

Table 3. Evaluation between the process used in this research and similar studies using some of the extraction procedures.

Adsorbent	LOD[a]	P.F[b]	Refs.[c]
Agar powder modified with 2-mercaptobenzimidazole	0.02	100	[4]
Octadecyl silica cartridge with 4-bpdb	1.87×10^{-3}	128	[36]
Cloud point extraction(using surfactant Triton X-114)	5×10^{-3}	29	[45]
Ion-imprinted thiol-functionalized silica gel	0.35	75	[46]
Surfactant-sensitized spectrophotometric	6	-	[47]
p-sulfobenzylidenerhodanine (SBDR) & C18 cartridge	0.02	50	[48]
Spectrophotometric determination (o-carboxy phenyl diazoamino p-azobenzene)	80	-	[49]
Cation-exchanger Dowex 50Wx4	0.027	-	[50]
Silica C18 modified	2.5×10^{-4}	-	[51]
Silica gel immobilized amines 2-thiophenecarboxaldehyde	4.75×10^{-3}	-	[52]
Modified octadecyl silica membrane	3.8×10^{-3}	500	[53]
Spectrophotometric determination (cellulose column)	2	33	[54]
Methylmercury-imprinted polymers	0.041	-	[55]
Silica gel-loaded dithizone phases	0.02	200	[56]
Silica-coated magnetic nanoparticles modified	1.07×10^{-4}	-	[57]
Silica gel modified with diaminothiourea	0.28	-	[58]
Sodium dodecyle sulphate-coated magnetite nanoparticles	0.04	1230	[59]
Cloud point extraction(non-ionic surfactant Triton X-114)	4×10^{-3}	42	[60]
liquid–liquid extraction	2.3×10^{-3}	36	[61]
Hg(II)-imprinted thiol-functionalized mesoporous sorbent	0.39	150	[62]
Ghezeljeh montmorillonite nanoclay	0.033	9	Present work

[a] LOD, limit of detection (ng/mL).[b] P.F, preconcentration factor.[c] Ref., reference.

then an equivalent quantity of *Ghezeljeh* nanoclay (1 g) was added into each bottle at the required temperature, immediately, adsorption of mercury ions on *Ghezeljeh* nanoclay was investigated after 5, 10, 15, 20, 30, 40, 50, 100, 150, 200 and 300 min of shaking in incubator shaker. The resulting solutions were centrifuged and the supernatant liquids were subjected for the calculation of mercury ions. The concentration of metal ions residue in the solution was determined by taking the difference of primary and final metal ion concentrations (Fig. 3). Adsorption procedure was calculated by computing the sorption percentage (Adsorption %) as determined by the following:

$$\text{Adsorption\%}=\frac{(C_0 - C_e)}{C_0}\times100 \tag{1}$$

where C_0 is the primary concentration and C_e is the equilibrium concentration, mg/l. The quantity of ions adsorbed per unit mass of adsorbed, q_e (mg/g) is estimated by the subsequent expression:

$$q_e=\frac{C_0-C_e}{w\times V} \tag{2}$$

at which V(ml) is the volume of metal ions solution, and w (mg) is the weight of adsorbent. Adsorption isotherm displays the correlation between the adsorption capacity (q_e) and the equilibrium concentration (C_e) of ions in the liquid part.

As shown in (Fig. 3), at lesser concentrations, a great amount of adsorption positions on the nanoclay are obtainable for the metal ions and this condition is altered with the addition of metal ion concentration and the competition for adsorption positions gets hard. Adsorption isotherm, at consistent temperature, displays the correlation between the adsorption capacity (q_e) and the equilibrium concentration (C_e) of ions in the liquid part. Adsorption isotherm models are commonly applied for fitting the data, and give essential information about the mechanism of adsorption and support us in the plan of new adsorbing structures [40]. In this research, the isotherm data was analyzed by the Temkin, Dubinin–Radushkevich, Langmuir, and Freundlich equations.

Langmuir isotherm

The Langmuir equation is frequently applied to explain adsorption of solute from liquid solutions, and its corresponding model accepts the monolayer presentation of the adsorption surface with a finite number of adsorption sites, by monolayer adsorption without any interaction between adsorbed molecules and is expressed by the subsequent equation [37].

$$\frac{C_e}{q_e}=\frac{1}{K_L q_m}+\frac{C_e}{q_m} \tag{3}$$

Values of q_m and K_L are evaluated from the plot of *(C_e/q_e) verses (1/C_e)*. C_e is the equilibrium

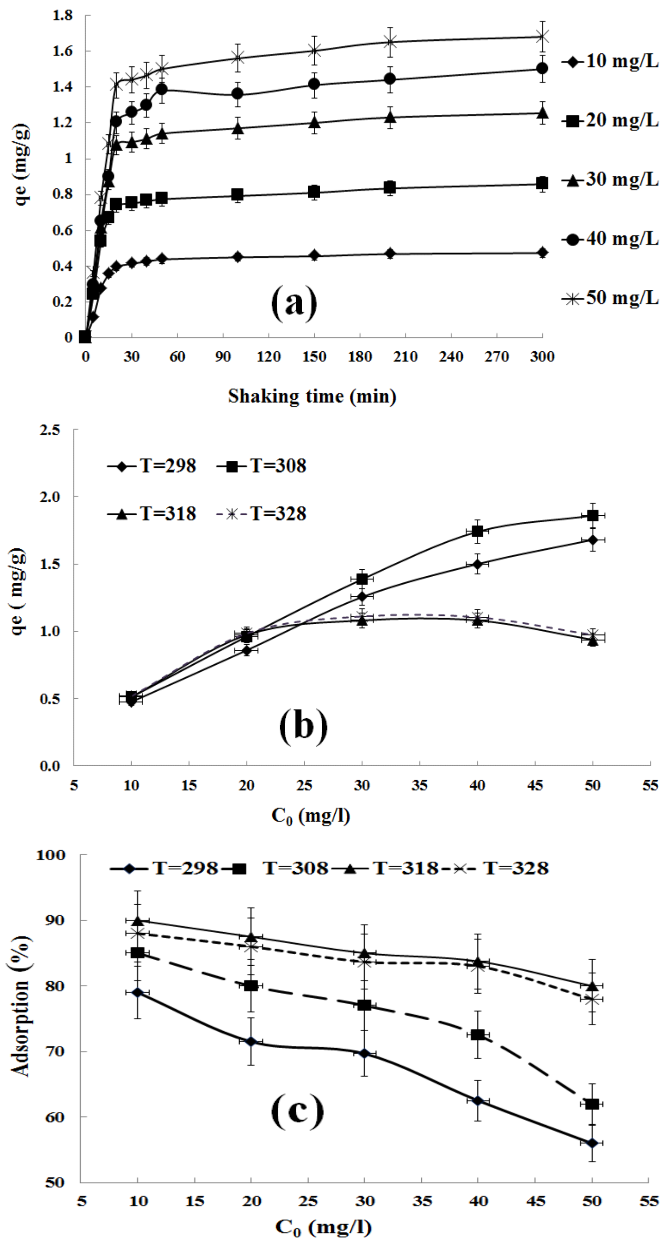

Fig. 3. Effect of (a) shaking time, and (b) initial concentration on the adsorption capacity in different temperatures. (c) Effect of initial concentration in different temperatures on the adsorption percentage of mercury ion onto *Ghezeljeh* nanoclay.

concentration of metal ions onto the adsorbent (mg/L), q_e is the quantity of metal ions adsorbed per unit quantity of nanoclay at equilibrium concentration (mg/g), q_m (mg/g) is the extreme adsorption capacity, and K_L is Langmuir constant correlated for sorption energy; specifically, K_L displays adsorption enthalpy which commonly differs with temperature [20]. The Langmuir isotherm was used to our investigational data and the results are revealed in Fig. 4a and Table 4. One of the critical factors of Langmuir equation is the equilibrium or separation factor (R_L) (Fig. 4b). R_L can be determined by the subsequent equation:

$$R_L = \frac{1}{1+K_L C_0} \tag{4}$$

where C_0 (mg/L) is the maximum primary solute concentration. The R_L indicates the kind of isotherm being acceptable ($0 < R_L < 1$) or unacceptable ($R_L > 1$) or irreversible ($R_L = 0$) [41]. This parameter indicated that nanoclay is an appropriate adsorbent for the adsorption of mercury ions from aqueous solutions.

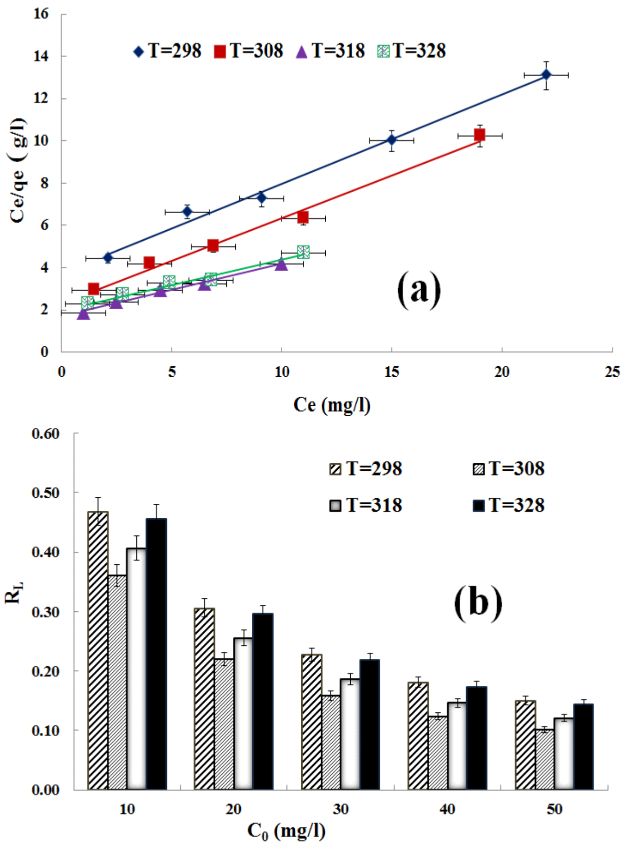

Fig. 4. (a) Langmuir isotherm, and (b) separation factor for adsorption of mercury ions on *Ghezeljeh* nanoclay.

Freundlich isotherm

The Freundlich isotherm model confirms that the surface is dissimilar and the energy of sorption is not consistent. This model moreover accepts the multilayer adsorption. The linear formula of the Freundlich equation is specified in the subsequent equation [20,41],

$$\log q_e = \log K_F + \frac{1}{n}\log C_e \quad (5)$$

where q_e explains the quantity of metal species adsorbed at equilibrium in mg/g, C_e is the solute equilibrium concentration in mg/l, K_F and n are Freundlich consistents correlated to the adsorption capacity and intensity of adsorption, respectively. K_F and n were defined from plot of *log* q_e *verses log* C_e (Table 4). A satisfactory adsorption has n values in the range of 1–10; for this research, we established a favorable value for *n*.

Dubinin–Radushkevich isotherm

The Dubinin–Radushkevich isotherm is extra general since it does not accept a uniform surface or consistent sorption potential. It is applied to discriminate between the physical and chemical adsorption of metal ions on surfaces [40]. The Dubinin–Radushkevich calculation is known by Eq. (6):

$$\ln q_e = \ln q_m - k\varepsilon^2 \quad (6)$$

where q_e and q_m have the equal significance as before, k (mol^2/J^2) is a consistent correlated to the adsorption energy, and ε is the extreme adsorption capability known by Eq. (7):

$$\varepsilon = RT\ln\left(1+\frac{1}{C_e}\right) \quad (7)$$

R (J/mol K) is the gas constant, and *T* (K) is the absolute temperature. The constant *k* gives the mean free energy *E* (kJ/mol) of sorption per molecule of the sorbate when it is carried to the surface of the solid from an infinite distance in the solution and can be calculated using Eq. (8) and is applied to evaluate the kind of adsorption process. If $E < 8$ kJ/mol, adsorption procedure is of a physical nature while, if value $8 < E < 16$ kJ/mol, the adsorption procedure can be described by ion interchange mechanism.

$$E = \frac{1}{(-2k)^{\frac{1}{2}}} \tag{8}$$

In this research, small values of E show that the adsorption procedure is a physical nature (Table 4).

Temkin Isotherm

Temkin and Pyzhev [42] evaluated the properties of some indirect adsorbate/adsorbate interactions onto adsorption isotherms. They proposed, regardless the concentration of these adsorbates, their interactions cause that the heat of adsorption of all molecules in the layer would reduce linearly with coverage. The derivation of the Temkin isotherm accepts that the reduction in the heat of sorption is more linear rather than logarithmic, as indicated in the Freundlich equation [33]. The Temkin isotherm has been frequently used in the subsequent formula:

$$q_e = \frac{RT}{b}\ln(K_T C_e) \tag{9}$$

$$q_e = A + B\ \ln C_e \tag{10}$$

$$A = \frac{RT}{b}\ln K_T \tag{11}$$

where $B = RT/b$, R is gas constant (8.314 J/mol K), T is the temperature (K), K_T is equilibrium binding constant (L/g); b is correlated to heat of adsorption (J/mol). The sorption data can be investigated using Eq. (10). Consequently, a plot of q_e *versus* $\ln C_e$ permits one to define the consistent as shown in Table 4.

Data from Fig. 4 and Table 4 show that Langmuir and Freundlich model acceptably fit the experimental data for mercury ions.

Adsorption kinetics

To estimate the kinetic mechanism for the adsorption of mercury ions on *Ghezeljeh* nanoclay, and its potential rate-controlling stages that comprise mass transport and chemical reaction procedures, kinetic models similar to pseudo-first-order, pseudo-second-order, and intra-particle diffusion were examined [43].

Pseudo-first-order model

Pseudo- first-order model was commonly explained as follows [44]:

$$\log(q_e - q_t) = \log q_e - \frac{k_1 t}{2.303} \tag{12}$$

where q_e is the quantity of metal ions adsorbed per unit mass of adsorbent at equilibrium i.e., adsorption capacity (mg/g), q_t is the quantity of adsorbent adsorbed (mg/g) at any time t and k_1 is the rate constant. The value of k_1 was computed from the slope of the linear plot of $\log(q_e - q_t)$ *versus* t (Table 5).

Pseudo-second-order rate model

Pseudo-second-order rate model is known as follows:

$$\frac{t}{q_t} = \frac{1}{k_2 q_e^2} + \frac{t}{q_e} \tag{13}$$

where k_2 is the rate constant. The values of k_2 can be computed from the plot of t / q_t *versus* t; see Fig. 5a, and Table 5.

Intra-particle diffusion model (Waber–Morris model)

To define the rate-controlling stage, intraparticle diffusion model was used to adsorption kinetic data as known via the subsequent equation [38,39].

$$q_t = k_{int} t^{\frac{1}{2}} \tag{14}$$

Table 4. Langmuir, Freundlich, Dubinin-Radushkevich and Temkin isotherms parameters.

Temperature(K)	Langmuir constants					Freundlich constants		
	q_e (mg/g)	K_L (L/mg)	q_m	R^2	R_L	K_F (mg/g)	1/n	R^2
298	0.474	0.113	2.365	0.991	0.468	0.327	0.555	0.978
308	0.510	0.177	2.466	0.990	0.361	0.426	0.567	0.980
318	0.540	0.1456	4.037	0.988	0.407	0.543	0.697	0.999
328	0.530	0.119	4.182	0.983	0.456	0.463	0.757	0.998

Temperature(K)	Dubinin-Radushkevich constant				Temkin constants		
	k (mol^2/J)	q_m	E (J/mol)	R^2	K_{Te} (L/g)	b_{Te} (kJ/mol)	R^2
298	1.123	1.304	0.667	0.887	0.979	1.336	0.984
308	0.697	1.596	0.846	0.887	1.584	4.508	0.977
318	0.400	1.929	1.118	0.876	1.846	3.476	0.967
328	0.5003	1.927	0.999	0.889	1.457	3.355	0.964

Table 5. Adsorption kinetics models and thermodynamic parameters of Hg(II) ions adsorption.

C_0 (mg/L)	Pseudo first order kinetic model			Pseudo second order kinetic model			Intraparticle diffusion	
	K_1	q_e (mg/g)	R^2	K_2	q_e (mg/g)	R^2	K_{int} (mg/g $min^{1/2}$)	R^2 (t≤20min)
10	0.0179	0.178	0.809	0.324	0.483	0.9984	0.093	0.948
20	0.0138	0.292	0.704	0.193	0.865	0.9986	0.173	0.960
30	0.0163	0.492	0.777	0.106	1.278	0.9981	0.239	0.942
40	0.0138	0.635	0.705	0.068	1.529	0.9966	0.261	0.923
50	0.0168	0.726	0.813	0.0689	1.719	0.9976	0.309	0.931

C_0(mg/L)	Temperature (K)	ΔS^o (kJ/mol K)	ΔH^o(kJ/mol)	ΔG^o (kJ/mol)
10	298	0.102	34.328	3.69
	308			2.76
	318			1.63
20	298	0.118	40.240	4.691
	308			4.037
	318			2.293
30	298	0.120	40.845	4.910
	308			4.110
	318			2.852
40	298	0.129	44.366	5.705
	308			4.722
	318			3.103
50	298	0.129	45.043	6.373
	308			5.274
	318			3.773

where q_t is the quantity of metal ions adsorbed onto nanoclay at time *t*, and k_{int} is the rate constant for intraparticle diffusion. Fig. 5b displays a plot of q_t *verses* $t^{1/2}$. It may show multi-linearity which displays two or more stages occurring in the adsorption procedure. The first sharper part ($t \leq 20$ min) is the outside surface adsorption or instant adsorption step. The second part is the slow adsorption step where the intraparticle diffusion rate is measured. The third is the ending equilibrium step where intraparticle diffusion begins to slow down because of enormously small solute concentration in the solution. The factors computed are brought in Table 5. The quantity of k_{int} was superior at the greater concentrations. The multi-stepped adsorption detected for all the metal ions and finest fitting found for the investigational data in height regression coefficient quantities shows that pseudo second order kinetic model might play an important role in the adsorption of metal ions onto nanoclay.

Determination of thermodynamic parameters

Three thermodynamic factors free energy change (ΔG^0) enthalpy change (ΔH^0) and entropy change (ΔS^0) were computed by the subsequent equations:

$$k_L = \frac{q_e}{C_e} \tag{15}$$

$$\Delta G^0 = - RT\ln k_L \tag{16}$$

$$\ln k_L = \frac{\Delta S^0}{R} - \frac{\Delta H^0}{RT} \tag{17}$$

$$\Delta S^0 = \frac{\Delta H^0 - \Delta G^0}{T} \tag{18}$$

where *R* is the universal gas constant, 8.314 J/mol K, *T* is the absolute temperature (K), and k_L is the Langmuir constant (mol/l). ΔS^0 and ΔH^0 could be found from the slope and intercept of *ln* k_L *versus* $1/T$ according to the equation (17). Quantities of ΔS^0, ΔH^0 and ΔG^0 are displayed in Table 5. The positive values of ΔH° confirm the endothermic nature of the sorption procedure. As clearly shown in Table 5, the positive quantities of ΔG^0 is decreased with the rise of sorption temperature, indicating the superior sorption at upper temperature. Also, the positive quantities of entropy change (ΔS^0) show that the randomness at the solid–liquid boundary throughout the adsorption procedure increases. The small enthalpy quantities of ΔH° < 20 kJ/mol show that the physisorption is involved in the procedure of adsorption. The estimated quantities of ΔH° for the current system were greater than 20 kJ/mol and therefore, the procedure may include a spontaneous sorption mechanism as ion exchange where chemical links are not of powerful energies [44].

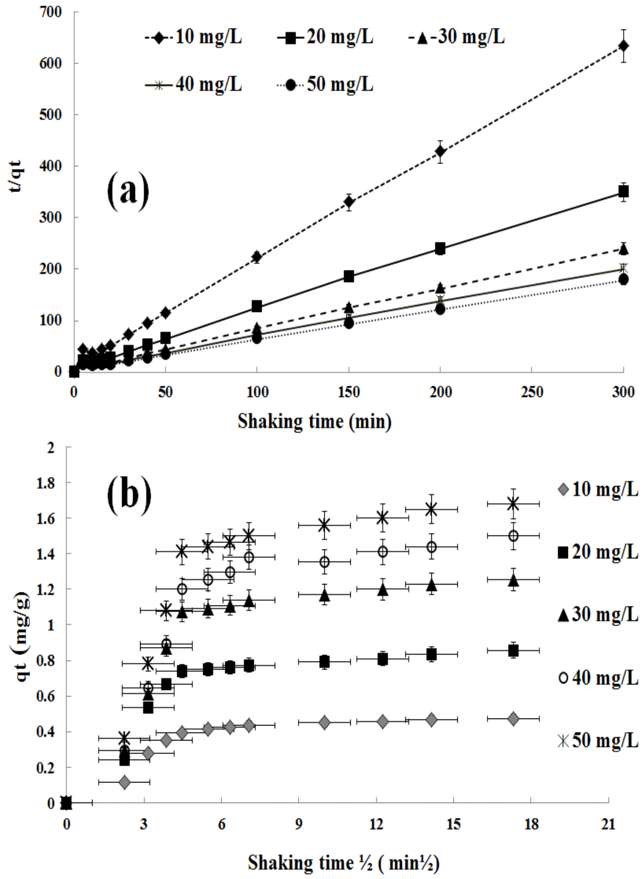

Fig. 5. (a) Pseudo second order kinetic model, and (b) intraparticle diffusion for mercury ions adsorption on *Ghezeljeh* nanoclay.

CONCLUSIONS

This research attempted to extract and preconcentrate mercury ions from aqueous solutions with the *Ghezeljeh* montmorillonite clay as a native adsorbent. To this end, the adsorbent was prepared using the *Galehouse* way and made distinctive via Fourier transform infrared spectroscopy (FT-IR), scanning electron microscopy-energy dispersive spectrometer operating (SEM-EDS), X-ray diffractometry (XRD), X-ray fluorescence (XRF), cation exchange capacity (CEC) measurements and specific surface area (S_{BET}). The results of XRD, FT-IR, zeta potential and CEC of the *Ghezeljeh* clay confirm that montmorillonite is the dominant mineral phase. On the basis of SEM images of clay, the distance between the plates is in nm level. A number of effective parameters on extraction-preconcentration were optimized using standard solutions. It was also shown that additional metal ions in the aqueous solution containing mercury ions generally do not have a negative effect on mercury ion recovery. The figures of merit were also calculated: LOD, 0.033 ng/ml; LOQ, 0.11 ng/ml; preconcentration factor, 9; DLR from 0.11 ng/ml to 22.2 μg/ml, and adsorption capacity of the clay was 1.17 mg/g. In the optimized standard solution, full recovery (100%) was obtained. At a later stage, the experimental process was used to a variety of natural water and fish samples under the optimized condition with the recovery being still significant. Good recoveries of spiked samples demonstrate the accuracy of the methods used. In addition, data show that Langmuir and Freundlich models acceptably fit the investigational data for mercury ions. Adsorption of mercury ions onto *Ghezeljeh* montmorillonite nanoclay obeyed the pseudo-second-order kinetic model. Calculation of ΔG^0, ΔH^0 and ΔS^0 displayed that the nature of mercury ions sorption is endothermic and favorable at upper temperature.

CONFLICT OF INTEREST

The authors declare that there is no conflict of interests regarding the publication of this paper.

ACKNOWLEDGEMENTS

The authors are grateful for the financial support of this work by the Imam Khomeini International University (IKIU), and Mines and Mining Industries Development and Renovation Organization of Iran (IMIDRO).

REFERENCES

1. Brigatti MF, Colonna S, Malferrari D, Medici L, Poppi L. Mercury adsorption by montmorillonite and vermiculite: a combined XRD, TG-MS, and EXAFS study. Applied Clay Science. 2005;28(1–4):1-8.
2. Manohar DM, Anoop Krishnan K, Anirudhan TS. Removal of mercury(II) from aqueous solutions and chlor-alkali industry wastewater using 2-mercaptobenzimidazole-clay. Water Research. 2002;36(6):1609-19.
3. Anirudhan TS, Bringle CD, Radhakrishnan PG. Heavy metal interactions with phosphatic clay: Kinetic and equilibrium studies. Chemical Engineering Journal. 2012;200–202:149-57.
4. Pourreza N, Ghanemi K. Determination of mercury in water and fish samples by cold vapor atomic absorption spectrometry after solid phase extraction on agar modified with 2-mercaptobenzimidazole. Journal of Hazardous Materials. 2009;161(2–3):982-7.
5. Dou B, Dupont V, Pan W, Chen B. Removal of aqueous toxic Hg(II) by synthesized TiO2 nanoparticles and TiO2/montmorillonite. Chemical Engineering Journal. 2011;166(2):631-8.
6. Sajidu SMI, Persson I, Masamba WRL, Henry EMT. Mechanisms of heavy metal sorption on alkaline clays from Tundulu in Malawi as determined by EXAFS. Journal of Hazardous Materials. 2008;158(2–3):401-9.
7. Soleimani M, Rafiei B, Siahpoosh ZH. Ghezeljeh montmorillonite nanoclay as a natural adsorbent for solid phase extraction of copper ions from food samples. Journal of Analytical Chemistry. 2015;70(7):794-803.
8. Soleimani M, Siahpoosh ZH. Ghezeljeh nanoclay as a new natural adsorbent for the removal of copper and mercury ions: Equilibrium, kinetics and thermodynamics studies. Chinese Journal of Chemical Engineering. 2015;23(11):1819-33.
9. Soleimani M, Siahpoosh ZH. Determination of Cu(II) in water and food samples by Na+-cloisite nanoclay as a new adsorbent: Equilibrium, kinetic and thermodynamic studies. Journal of the Taiwan Institute of Chemical Engineers. 2016;59:413-23.
10. Tyagi B, Chudasama CD, Jasra RV. Determination of structural modification in acid activated montmorillonite clay by FT-IR spectroscopy. Spectrochimica Acta Part A: Molecular and Biomolecular Spectroscopy. 2006;64(2):273-8.
11. Adhikari T, Singh MV. Sorption characteristics of lead and cadmium in some soils of India. Geoderma. 2003;114(1–2):81-92.
12. Mcbride MB. Environmental Chemistry of Soils. New York: Oxford University Press; 1994.
13. da Fonseca MG, de Oliveira MM, Arakaki LNH. Removal of cadmium, zinc, manganese and chromium cations from aqueous solution by a clay mineral. Journal of Hazardous Materials. 2006;137(1):288-92.
14. Coles CA, Yong RN. Aspects of kaolinite characterization and retention of Pb and Cd. Applied Clay Science. 2002;22(1–2):39-45.
15. Auboiroux M, Baillif P, Touray JC, Bergaya F. Fixation of Zn2+ and Pb2+ by a Ca-montmorillonite in brines and dilute solutions: Preliminary results. Applied Clay Science. 1996;11(2):117-26.
16. Breen C, Bejarano-Bravo CM, Madrid L, Thompson G, Mann BE. Na/Pb, Na/Cd and Pb/Cd exchange on a low iron Texas bentonite in the presence of competing H+ ion. Colloids and Surfaces A: Physicochemical and Engineering Aspects. 1999;155(2–3):211-9.
17. Bektaş N, Ağım BA, Kara S. Kinetic and equilibrium studies in removing lead ions from aqueous solutions by natural sepiolite. Journal of Hazardous Materials. 2004;112(1–2):115-22.
18. Echeverría JC, Zarranz I, Estella J, Garrido JJ. Simultaneous effect of pH, temperature, ionic strength, and initial concentration on the retention of lead on illite. Applied Clay Science. 2005;30(2):103-15.
19. Gu X, Evans LJ, Barabash SJ. Modeling the adsorption of Cd (II), Cu (II), Ni (II), Pb (II) and Zn (II) onto montmorillonite. Geochimica et Cosmochimica Acta. 2010;74(20):5718-28.
20. Erdem E, Karapinar N, Donat R. The removal of heavy metal cations by natural zeolites. Journal of Colloid and Interface Science. 2004;280(2):309-14.
21. Tansel B, Sager J, Rector T, Garland J, Strayer RF, Levine L, et al. Significance of hydrated radius and hydration shells on ionic permeability during nanofiltration in dead end and cross flow modes. Separation and Purification Technology. 2006;51(1):40-7.
22. Krishnan KA, Anirudhan TS. Uptake of Heavy Metals in Batch Systems by Sulfurized Steam Activated Carbon Prepared from Sugarcane Bagasse Pith. Industrial & Engineering Chemistry Research. 2002;41(20):5085-93.
23. Sen Gupta S, Bhattacharyya KG. Immobilization of Pb(II), Cd(II) and Ni(II) ions on kaolinite and montmorillonite surfaces from aqueous medium. Journal of Environmental Management. 2008;87(1):46-58.
24. Novaković T, Rožić L, Petrović S, Rosić A. Synthesis and characterization of acid-activated Serbian smectite clays obtained by statistically designed experiments. Chemical Engineering Journal. 2008;137(2):436-42.
25. Uddin F. Clays, Nanoclays, and Montmorillonite Minerals. Metallurgical and Materials Transactions A. 2008;39(12):2804-14.
26. Rafiei B, Amini Manesh A. Mineralogy of shampoo-clay deposit in Tafresh area, central province. GeoSci. 2007;16(63):180-3.
27. H. Van Olphen JJF. Data Handbook for Clay Materials and other Nonmetallic Minerals. New York: Pergamon Press; 1979.
28. MEIER, P. L, KAHR, G. Determination of the cation exchange capacity (CEC) of clay minerals using the complexes of copper(II) ion with triethylenetetramine and tetraethylenepentamine. Chantilly, VA, ETATS-UNIS: Clay Minerals Society; 1999.

29. Ammann L, Bergaya F, Lagaly G. Determination of the cation exchange capacity of clays with copper complexes revisited. Clay Minerals2005. p. 441.
30. Grim RE. Clay Mineralogy. New York: McGraw-Hill; 1968.
31. Eren E, Afsin B. An investigation of Cu(II) adsorption by raw and acid-activated bentonite: A combined potentiometric, thermodynamic, XRD, IR, DTA study. Journal of Hazardous Materials. 2008;151(2–3):682-91.
32. Errais E, Duplay J, Darragi F, M'Rabet I, Aubert A, Huber F, et al. Efficient anionic dye adsorption on natural untreated clay: Kinetic study and thermodynamic parameters. Desalination. 2011;275(1–3):74-81.
33. Adebowale KO, Unuabonah IE, Olu-Owolabi BI. The effect of some operating variables on the adsorption of lead and cadmium ions on kaolinite clay. Journal of Hazardous Materials. 2006;134(1–3):130-9.
34. Bhattacharyya KG, Gupta SS. Adsorptive accumulation of Cd(II), Co(II), Cu(II), Pb(II), and Ni(II) from water on montmorillonite: Influence of acid activation. Journal of Colloid and Interface Science. 2007;310(2):411-24.
35. Bhattacharyya KG, Gupta SS. Removal of Cu(II) by natural and acid-activated clays: An insight of adsorption isotherm, kinetic and thermodynamics. Desalination. 2011;272(1–3):66-75.
36. Demirel S, Tuzen M, Saracoglu S, Soylak M. Evaluation of various digestion procedures for trace element contents of some food materials. Journal of Hazardous Materials. 2008;152(3):1020-6.
37. Malamis S, Katsou E. A review on zinc and nickel adsorption on natural and modified zeolite, bentonite and vermiculite: Examination of process parameters, kinetics and isotherms. Journal of Hazardous Materials. 2013;252–253:428-61.
38. Ho Y-S. Isotherms for the sorption of lead onto peat: comparison of linear and non-linear methods. Polish journal of environmental studies. 2006;15(1):81-6.
39. Ho Y-S. Review of second-order models for adsorption systems. Journal of Hazardous Materials. 2006;136(3):681-9.
40. Ghasemi Z, Seif A, Ahmadi TS, Zargar B, Rashidi F, Rouzbahani GM. Thermodynamic and kinetic studies for the adsorption of Hg(II) by nano-TiO2 from aqueous solution. Advanced Powder Technology. 2012;23(2):148-56.
41. Rashidi F, Sarabi RS, Ghasemi Z, Seif A. Kinetic, equilibrium and thermodynamic studies for the removal of lead (II) and copper (II) ions from aqueous solutions by nanocrystalline. Superlattices and Microstructures. 2010;48(6):577-91.
42. Temkin M, Pyzhev V. Kinetics of ammonia synthesis on promoted iron catalysts. Acta physiochim URSS. 1940;12(3):217-22.
43. Sheela T, Nayaka YA. Kinetics and thermodynamics of cadmium and lead ions adsorption on NiO nanoparticles. Chemical Engineering Journal. 2012;191:123-31.
44. Smičiklas I, Onjia A, Raičević S, Janaćković Đ, Mitrić M. Factors influencing the removal of divalent cations by hydroxyapatite. Journal of Hazardous Materials. 2008;152(2):876-84.
45. Soleimani M, Mahmodi MS, Morsali A, Khani A, Afshar MG. Using a new ligand for solid phase extraction of mercury. Journal of Hazardous Materials. 2011;189(1–2):371-6.
46. Yuan C-G, Lin K, Chang A. Determination of trace mercury in environmental samples by cold vapor atomic fluorescence spectrometry after cloud point extraction. Microchimica Acta. 2010;171(3):313-9.
47. Wang Z, Wu G, He C. Ion-imprinted thiol-functionalized silica gel sorbent for selective separation of mercury ions. Microchimica Acta. 2009;165(1):151-7.
48. Gürkan R, Çepken T, Ulusoy HI. Surfactant-sensitized spectrophotometric determination of Hg (II) in water samples using 2-(2-thiazolylazo)-p-cresol as ligand and cetylpyridinium chloride as cationic surfactant. Turkish Journal of Chemistry. 2012;36(1):159-77.
49. Zhang Y, Yang G, Hu Q, Jiayuan Y, Li Z. Solid Phase Extraction and Spectrophotometric Determination of Mercury in Tobacco and Tobacco Additives with p-Sulfobenzylidenerhodanine as Chromogenic Reagent. Microchimica Acta. 2004;146(3):297-302.
50. Chatterjee S, Pillai A, Gupta VK. Spectrophotometric determination of mercury in environmental sample and fungicides based on its complex with o-carboxy phenyl diazoamino p-azobenzene. Talanta. 2002;57(3):461-5.
51. Krata A, Pyrzyńska K, Bulska E. Use of solid-phase extraction to eliminate interferences in the determination of mercury by flow-injection CV AAS. Analytical and Bioanalytical Chemistry. 2003;377(4):735-9.
52. Segade SR, Tyson JF. Determination of methylmercury and inorganic mercury in water samples by slurry sampling cold vapor atomic absorption spectrometry in a flow injection system after preconcentration on silica C18 modified. Talanta. 2007;71(4):1696-702.
53. Soliman EM, Saleh MB, Ahmed SA. New solid phase extractors for selective separation and preconcentration of mercury (II) based on silica gel immobilized aliphatic amines 2-thiophenecarboxaldehyde Schiff's bases. Analytica Chimica Acta. 2004;523(1):133-40.
54. Ashkenani H, Dadfarnia S, Shabani AMH, Jaffari AA, Behjat A. Preconcentration, speciation and determination of ultra trace amounts of mercury by modified octadecyl silica membrane disk/electron beam irradiation and cold vapor atomic absorption spectrometry. Journal of Hazardous Materials. 2009;161(1):276-80.
55. Rajesh N, Hari MS. Spectrophotometric determination of inorganic mercury (II) after preconcentration of its diphenylthiocarbazone complex on a cellulose column. Spectrochimica Acta Part A: Molecular and Biomolecular Spectroscopy. 2008;70(5):1104-8.
56. Liu Y, Zai Y, Chang X, Guo Y, Meng S, Feng F. Highly selective determination of methylmercury with methylmercury-imprinted polymers. Analytica Chimica Acta. 2006;575(2):159-65.
57. Mahmoud ME, Osman MM, Amer ME. Selective pre-concentration and solid phase extraction of mercury(II) from natural water by silica gel-loaded dithizone phases. Analytica Chimica Acta. 2000;415(1–2):33-40.
58. Huang C, Hu B. Silica-coated magnetic nanoparticles modified with γ-mercaptopropyltrimethoxysilane for fast and selective solid phase extraction of trace amounts of Cd, Cu, Hg, and Pb in environmental and biological samples prior to their determination by inductively coupled plasma mass spectrometry. Spectrochimica Acta Part B: Atomic Spectroscopy. 2008;63(3):437-44.
59. Wu Q, Chang X, He Q, Zhai Y, Cui Y, Huang X. Silica gel modified with diaminothiourea as selective solid-phase

extractant for determination of Hg(II) in biological and natural water samples. International Journal of Environmental Analytical Chemistry. 2008;88(4):245-54.

60. Faraji M, Yamini Y, Rezaee M. Extraction of trace amounts of mercury with sodium dodecyle sulphate-coated magnetite nanoparticles and its determination by flow injection inductively coupled plasma-optical emission spectrometry. Talanta. 2010;81(3):831-6.

61. Chen H, Chen J, Jin X, Wei D. Determination of trace mercury species by high performance liquid chromatography–inductively coupled plasma mass spectrometry after cloud point extraction. Journal of Hazardous Materials. 2009;172(2–3):1282-7.

62. Martinis EM, Bertón P, Olsina RA, Altamirano JC, Wuilloud RG. Trace mercury determination in drinking and natural water samples by room temperature ionic liquid based-preconcentration and flow injection-cold vapor atomic absorption spectrometry. Journal of Hazardous Materials. 2009;167(1–3):475-81.